

RESEARCH ARTICLE

Tunable band structure and effective mass of disordered chalcopyrite

Ze-Lian Wang¹, Wen-Hui Xie², Yong-Hong Zhao^{1,†}

¹College of Physics and Electronic Engineering, Institute of Solid State Physics, Sichuan Normal University, Chengdu 610068, China

²Department of Physics, East China Normal University, Shanghai 200062, China

Corresponding author. E-mail: [†]yhzhao@sicnu.edu.cn

Received September 24, 2016; accepted November 1, 2016

The band structure and effective mass of disordered chalcopyrite photovoltaic materials $\text{Cu}_{1-x}\text{Ag}_x\text{GaX}_2$ ($X = \text{S}, \text{Se}$) are investigated by density functional theory. Special quasirandom structures are used to mimic local atomic disorders at Cu/Ag sites. A local density plus correction method is adopted to obtain correct semiconductor band gaps for all compounds. The bandgap anomaly can be seen for both sulfides and selenides, where the gap values of Ag compounds are larger than those of Cu compounds. Band gaps can be modulated from 1.63 to 1.78 eV for $\text{Cu}_{1-x}\text{Ag}_x\text{GaSe}_2$, and from 2.33 to 2.64 eV for $\text{Cu}_{1-x}\text{Ag}_x\text{GaS}_2$. The band gap minima and maxima occur at around $x = 0.5$ and $x = 1$, respectively, for both sulfides and selenides. In order to show the transport properties of $\text{Cu}_{1-x}\text{Ag}_x\text{GaX}_2$, the effective mass is shown as a function of disordered Ag concentration. Finally, detailed band structures are shown to clarify the phonon momentum needed by the fundamental indirect-gap transitions. These results should be helpful in designing high-efficiency photovoltaic devices, with both better absorption and high mobility, by Ag-doping in CuGaX_2 .

Keywords disorder, electronic structure, effective mass

PACS numbers 71.20.-b, 71.20.Nr

Although new photovoltaic materials, such as organic perovskites, have attracted much attention recently, [1–3] zinc-blende semiconductors still play an important role, owing to their high efficiency and stability in real environments. For example, $\text{Cu}_2\text{ZnSnSe}_4$ [4] (CZTS) and $\text{Cu}(\text{In}, \text{Ga})\text{Se}_2$ [5] (CIGS), which are both based on chalcopyrite CuGaX_2 ($X = \text{S}, \text{Se}$), have been considered as potential candidates for photovoltaics. It has been reported recently that the efficiency of CIGS has gone beyond 20%, which is close to that of polycrystalline silicon [6]. Furthermore, photovoltaic devices related to CZTS have gained attention because they solely contain abundant and nontoxic materials [4, 7].

The spectrum of sunshine arriving at the earth ranges from 0.35 to 2500 nm [8]. Therefore, tunable bandgaps are essential for photovoltaic materials, in order to absorb solar flux as much as possible. The use of doping impurities is the most commonly used method to modulate the bandgaps, as well as effective mass (EM), of

semiconductors [9–11]. Phase stability and formation energy of uniform impurities in CZTS have been systematically reviewed and classified using the supercell method [4, 12]. Owing to high manufacturing costs, practical photovoltaic devices cannot be made of crystalline CZTS, and hence atomic disordered defects and impurities are of high importance in practical devices. Although successful in uniform situations, the supercell method is difficult to apply to highly disordered impurities, which are very common in practical photovoltaic devices. In addition, the energy band structure is a key factor for both optical and electronic transport properties of photovoltaic materials. However, there is a well-known underestimation of semiconductor bandgaps by first-principles calculations. There are several common methods to modify the bandgap underestimation of density functional theory, such as the Heyd–Scuseria–Ernzerhof (HSE) hybrid functional [13], quasiparticle approximation with Green’s Function (GW) [14], and the modified Becke–Johnson (mBJ) [15] method. The HSE and GW calculations are extremely expensive in calcu-

*arXiv: 1612.03580.

lation, while the mBJ method can only give a partially corrected bandgap of 1.03 eV for CuGaSe_2 [16], which is still much smaller than the experimental value of 1.68 eV. Therefore, it is desirable to find a first-principles scheme to overcome the well-known bandgap underestimation for semiconductors, which is also capable of treating disordered impurities including spin-orbit coupling (SOC), with moderate computational cost.

Although CZTS and CIGS are the most important chalcopyrite photovoltaic materials, $\text{Cu}_{1-x}\text{Ag}_x\text{GaX}_2$ ($X = \text{Se}, \text{S}$) have also drawn much attention, owing to their interesting band anomalies and grain boundary effects [17–19]. In this work, we focus on the band structure and EM of $\text{Cu}_{1-x}\text{Ag}_x\text{GaX}_2$, modulated by disordered Ag atoms. The special quasirandom structure (SQS) method has been proved reasonable for disorder effects in all these compounds with x ranging from 0.0 to 1.0 [18, 20, 21]. The initial guesses of internal parameters are given by Ref. [18]. All electronic structure calculations are based on fully optimized SQS structures, including both lattice constants and internal parameters. The Vienna *ab-initio* simulation package is used for optimization, with the local density approximation (LDA) for exchange-correlation potential and projector augmented wave for pseudopotentials [22–24]. The kinetic energy cutoff for a plane wave basis is set to 800 eV and a k -mesh of $4 \times 4 \times 4$ is used. The optimized lattice constants are consistent with previous results for pure CuGaX_2 [25, 26] and AgGaX_2 [27], as listed in Table 1. It can be seen that sulfides have smaller lattice constants than selenides. For both sulfides and selenides, a increases with increasing Ag concentration, while there is a maximum value of c at approximately $x = 0.5$ and 0.75 for the sulfides and selenides, respectively. This indicates that there is a compression strain along the z -direction for all compounds when the Ag concentration is larger than the threshold value.

The electronic structure calculations are based on the linear combination of atomic orbital (LCAO) method as implemented in Nanodcal package [28–30]. A set of optimized double- ζ polarization (DZP) LCAO basis

Table 1 Full optimized lattice constants (a/c) of disordered $\text{Cu}_{1-x}\text{Ag}_x\text{GaX}_2$ ($X = \text{Se}, \text{S}$) given by SQS method in unit of Å.

x	$\text{Cu}_{1-x}\text{Ag}_x\text{GaSe}_2$	$\text{Cu}_{1-x}\text{Ag}_x\text{GaS}_2$
0.00	11.05/10.97	10.48/10.42
0.25	11.18/11.05	10.62/10.48
0.50	11.36/11.09	10.82/10.51
0.75	11.50/11.08	10.97/10.52
1.00	11.70/11.05	11.17/10.51

is used for all atoms, together with a real space grid energy cutoff of 300 Ry and a k -grid of $4 \times 4 \times 4$ in the first Brillouin zone. Self-consistent calculations are considered to be converged when the charge density has converged to less than 10^{-5} . In this work, we use a LDA plus correction method (LDA+C) [31] to modify the bandgaps of $\text{Cu}_{1-x}\text{Ag}_x\text{GaX}_2$. It is shown that experimental gap values can be achieved by choosing appropriate orbit-dependent correction parameters for each element, as given in Table 2. The calculated bandgaps for $\text{Cu}_{1-x}\text{Ag}_x\text{GaSe}_2$ and $\text{Cu}_{1-x}\text{Ag}_x\text{GaS}_2$ for $x = 0.0, 0.25, 0.5, 0.75,$ and 1.0 are shown in Fig. 1. Spin-orbit interaction is important for the electronic structure of semiconductors, which is included in all calculations. The solid red diamonds show the results including SOC, while the

Table 2 Orbit-dependent correction values in LDA+C calculation for all elements in $\text{Cu}_{1-x}\text{Ag}_x\text{GaX}_2$.

Element	s	p	d
Cu	0.00	0.00	4.73
Ag	0.00	0.00	5.46
Ga	3.00	0.00	0.00
Se	3.00	0.00	0.00
S	3.90	0.28	9.40

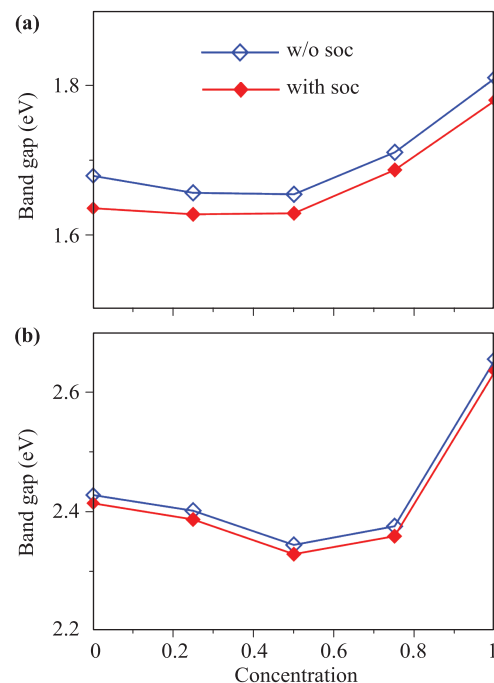


Fig. 1 Bandgaps as a function of Ag concentration, (a) for $\text{Cu}_{1-x}\text{Ag}_x\text{GaSe}_2$ and (b) for $\text{Cu}_{1-x}\text{Ag}_x\text{GaS}_2$. The blue hollow diamonds show that without SOC, while the red solid diamonds show that with SOC included.

hollow blue diamonds show those without SOC. It can be seen that there is a gap minimum for Ag concentration near 0.5 for both sulfides and selenides. The results show that SOC interaction can decrease the bandgaps significantly for selenides, but only modestly for sulfides. The calculated bandgaps are consistent with experimental [32] and semiclassical [18] values.

EM is important for the electronic transport properties in photovoltaic materials. Anisotropic EM is defined as follows:

$$m_i^* = \frac{\hbar^2}{d^2E/dk_i^2}, \quad i = x, y, z. \quad (1)$$

The calculated EM of $\text{Cu}_{1-x}\text{Ag}_x\text{GaSe}_2$ is shown in Fig. 2. These results indicate that EM behaves simi-

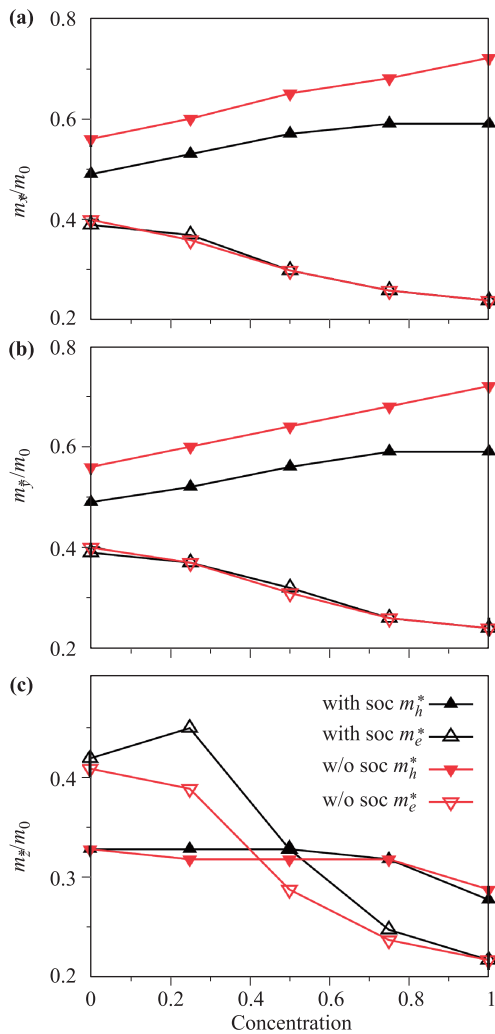


Fig. 2 Anisotropic EM of $\text{Cu}_{1-x}\text{Ag}_x\text{GaSe}_2$, where (a), (b), and (c) show the x -, y - and z -directions, respectively. In each subfigure, the solid and/or hollow triangles show hole and/or electron EM, respectively. The upward and downward triangles show those with and without SOC.

larly in the k_x - and k_y -directions, where the hole EM increases with Ag concentration and the electron EM decreases with it. Moreover, SOC can decrease the hole EM to approximately $0.07 m_0$, but keep the electron EM unchanged. Owing to the fact that the optimized lattice constants of SQSs deviate significantly from the cubic structure as given in Table 1, EM in the k_z -direction differs significantly from those in the k_x - and k_y -directions. The hole EM in the k_z -direction remains nearly constant for Ag concentration ranging from 0.0 to 0.75, and then decreases slightly until $x = 1.0$. However, the electron EM decreases remarkably with increasing Ag concentration. For $\text{Cu}_{1-x}\text{Ag}_x\text{GaS}_2$, there is a maximum at $x = 0.25$ and SOC has little effect on EM in the k_x - and k_y -directions. EM in the k_z -direction behaves similar to that of $\text{Cu}_{1-x}\text{Ag}_x\text{GaSe}_2$.

There are several type of EMs for different purposes, such as EM for density of states and conductivity, among others. For photovoltaic applications, EM for conductivity is of most importance, which is related to photocurrent and defined as follows:

$$m_{cond}^* = 3 \left(\frac{1}{m_x^*} + \frac{1}{m_y^*} + \frac{1}{m_z^*} \right)^{-1}. \quad (2)$$

The calculated m_{cond}^* as a function of Ag concentration is shown in Fig. 3. Figure 3(a) shows m_{cond}^* of $\text{Cu}_{1-x}\text{Ag}_x\text{GaSe}_2$. The hole EM increases slowly from $0.42m_0$ and reaches a maximum of $0.43m_0$ at approximately $x = 0.75$, while the electron EM quickly decreases from $0.40m_0$ to $0.23m_0$ with Ag concentration increasing from 0.0 to 1.0. m_{cond}^* of $\text{Cu}_{1-x}\text{Ag}_x\text{GaS}_2$ is shown in Fig. 3(b). The hole EM increases from $0.76m_0$ and reaches the maximum of $0.99m_0$ at approximately $x = 0.75$. The electron EM begins with $0.53m_0$ at $x = 0.0$, then reaches a maximum of $0.57m_0$ at approximately $x = 0.25$ and a minimum of $0.43m_0$ at $x = 1.0$. Generally speaking, a smaller EM implies a higher carrier mobility. Therefore, the electron mobility of $\text{Cu}_{1-x}\text{Ag}_x\text{GaSe}_2$ can be promoted by increasing Ag concentration, while accompanied by some reduction of hole mobility. For $\text{Cu}_{1-x}\text{Ag}_x\text{GaS}_2$, the electron mobility can be promoted only when the Ag concentration is larger than 0.25, and accompanied by a large reduction of hole mobility. On balance, the mobility of selenides is higher than that of sulfides for both electrons and holes, and should be enhanced by increased Ag concentration.

Optic absorption is one of the most important properties of photovoltaic materials. The optical transitions between any bands must obey conservation of both energy and momentum. Indirect-gap semiconductors undergo a phonon-assisted transition. However, for fundamental transition of direct-gap semiconductors, phonons are unnecessary, which typically results in higher absorption. On the other hand, direct bandgap will unfortunately

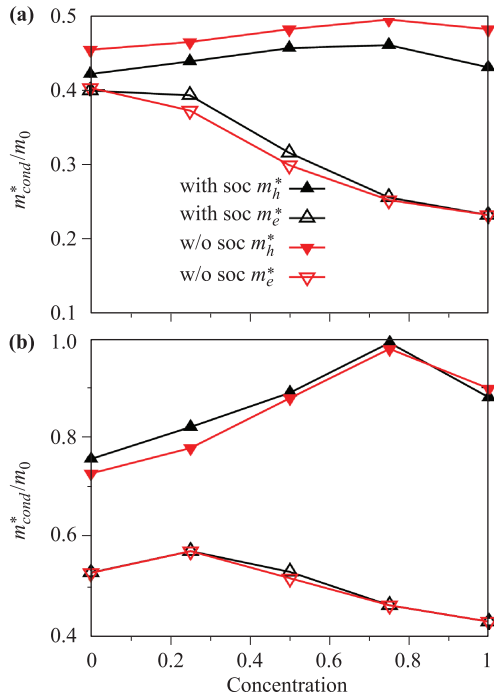


Fig. 3 EM for conductivity of (a) $\text{Cu}_{1-x}\text{Ag}_x\text{GaSe}_2$ and (b) $\text{Cu}_{1-x}\text{Ag}_x\text{GaS}_2$, where the upward and downward solid triangles show hole EM for with and without SOC, and hollow triangles for electron EM.

result in short minority carrier lifetime. The detailed band structure of $\text{Cu}_{1-x}\text{Ag}_x\text{GaSe}_2$ is shown in Fig. 4, where Δk_i^C ($i = x, y, z$) shows the deviation of the conduction band minimum (CBM) and Δk_i^V indicates the deviation of the valence band maximum (VBM) from the Γ point. $\Delta q_i = \Delta k_i^C - \Delta k_i^V$ is the phonon momentum needed by the fundamental indirect-gap transition. It can be seen from Figs. 4(a) and (b) that SOC causes the top valence band in the k_x -direction of CuGaSe_2 to split about 0.005 Bohr^{-1} , but leaves the bottom conduction band unsplit. Figure 4(c) shows Δq_x as a function of Ag concentration, which indicates that a larger phonon momentum is needed for larger Ag concentration compounds. The band structure in the k_y -direction is absolutely similar to that in the k_x -direction. The CBM and VBM of CuGaSe_2 in the k_z -direction are different and shown in Figs. 4(d) and (e), where it can be seen that VBM remains in the Γ point, regardless of SOC or an increase in Ag concentration. When there is no Ag, SOC causes a splitting of CBM, which disappears quickly with increasing Ag concentration. This means that a reduction of Ag ions can lead to a direct bandgap in the k_z -direction of $\text{Cu}_{1-x}\text{Ag}_x\text{GaSe}_2$.

In summary, we calculate the electronic band structure and effective mass of disordered quaternary chalcopyrite $\text{Cu}_{1-x}\text{Ag}_x\text{GaX}_2$ ($X = \text{Se}, \text{S}$) as a function of Ag concen-

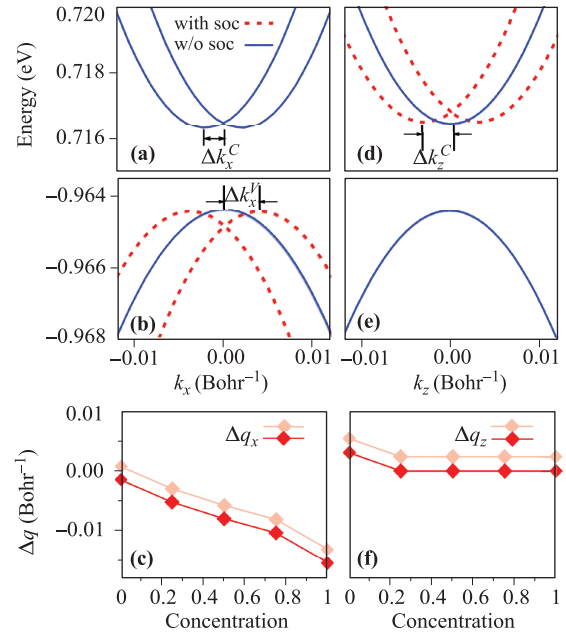


Fig. 4 Anisotropic band structure of $\text{Cu}_{1-x}\text{Ag}_x\text{GaSe}_2$, where (a) and (b) for conduction bands and valence bands in the k_x -direction, respectively. The blue lines show bands without SOC, while the red dot line those including SOC. (d) and (e) show band structure in k_z -direction. The momentum of phonon needed by fundamental transitions in the k_x - and k_z -directions are presented in (c) and (f).

tration. Disorder structures are depicted by SQS method and a LDA+C potential is used to correct the well-known bandgap underestimation of the first-principles calculation. SOC is included for all compounds. For both sulfides and selenides, the bandgap minimum appears at 50% Ag concentration. Meanwhile, bandgaps of AgGaX_2 are bigger than CuGaX_2 , which is consistent with the abnormal band structure of the previous study. The anisotropic EMs of $\text{Cu}_{1-x}\text{Ag}_x\text{GaX}_2$ have been calculated, from which the conductivity related to EM can be derived. The results show that the electron EM of $\text{Cu}_{1-x}\text{Ag}_x\text{GaSe}_2$ decreases with increasing Ag concentration, and the hole EM remains nearly constant. However, there are clear maxima at $x = 0.25$ and 0.75 for the electron and hole EM, respectively, of $\text{Cu}_{1-x}\text{Ag}_x\text{GaS}_2$. Moreover, the phonon momentum needed by fundamental indirect-gap transition will be increased substantially in the k_x - and k_y -directions by increased Ag concentration. Therefore, absorption along the k_x - and k_y -directions can be reduced by increased Ag concentration. In contrast, the bandgap in the k_z -direction becomes direct and the corresponding phonon momentum quickly goes to zero as the Ag concentration approaches 25%. Therefore, we deduce that absorption will be much more efficient in the k_z -direction than in the

k_x - and k_y -directions. Our calculated results will be useful in designing high-performance photovoltaic devices.

Acknowledgements We thank National Natural Science Foundation of China (Grant Nos. 11104191 and 51572086) and Sichuan Normal University for financial support.

References

- N. J. Jeon, J. H. Noh, Y. C. Kim, W. S. Yang, S. Ryu, and S. Seok, Solvent engineering for high-performance inorganic–organic hybrid perovskite solar cells, *Nat. Mater.* 13(9), 897 (2014)
- M. Liu, M. B. Johnston, and H. J. Snaith, Efficient planar heterojunction perovskite solar cells by vapour deposition, *Nature* 501(7467), 395 (2013)
- H. Zhou, Q. Chen, G. Li, S. Luo, T. Song, H. Duan, Z. Hong, H. You, Y. Liu, and Y. Yang, Interface engineering of highly efficient perovskite solar cells, *Science* 345(6196), 542 (2014)
- S. Chen, A. Walsh, X. G. Gong, and S. H. Wei, Classification of lattice defects in the kesterite $\text{Cu}_2\text{ZnSnS}_4$ and $\text{Cu}_2\text{ZnSnSe}_4$ earth-abundant solar cell absorbers, *Adv. Mater.* 25(11), 1522 (2013)
- M. G. Panthani, V. Akhavan, B. Goodfellow, J. P. Schmidtke, L. Dunn, A. Dodabalapur, P. F. Barbara, and B. A. Korgel, Synthesis of CuInS_2 , CuInSe_2 , and $\text{Cu}(\text{In}_x\text{Ga}_{1-x})\text{Se}_2$ (CIGS) nanocrystal “inks” for printable photovoltaics, *J. Am. Chem. Soc.* 130(49), 16770 (2008)
- M. A. Green, K. Emery, Y. Hishikawa, W. Warta, and E. D. Dunlop, Solar cell efficiency tables (Version 45), *Prog. Photon.: Res. Appl.* 23(1), 1 (2015)
- S. Abermann, Non-vacuum processed next generation thin film photovoltaics: Towards marketable efficiency and production of CZTS based solar cells, *Sol. Energy* 94, 37 (2013)
- T. P. Otanicar, I. Chowdhury, R. Prasher, and P. E. Phelan, Band-gap tuned direct absorption for a hybrid concentrating solar photovoltaic/thermal system, *J. Sol. Energy Eng.* 133(4), 041014 (2011)
- B. E. Sernelius, K. F. Berggren, Z. C. Jin, I. Hamberg, and C. G. Granqvist, Band-gap tailoring of ZnO by means of heavy Al doping, *Phys. Rev. B* 37(17), 10244 (1988)
- X. Nie, S. H. Wei, and S. B. Zhang, Bipolar doping and band-gap anomalies in delafossite transparent conductive oxides, *Phys. Rev. Lett.* 88(6), 066405 (2002)
- M. Cardona, Electron effective masses of InAs and GaAs as a function of temperature and doping, *Phys. Rev.* 121(3), 752 (1961)
- J. Pohl and K. Albe, Intrinsic point defects in CuInSe_2 and CuGaSe_2 as seen via screened-exchange hybrid density functional theory, *Phys. Rev. B* 87(24), 245203 (2013)
- A. V. Krukau, O. A. Vydrov, A. F. Izmaylov, and G. E. Scuseria, Influence of the exchange screening parameter on the performance of screened hybrid functionals, *J. Chem. Phys.* 125(22), 224106 (2006)
- M. S. Hybertsen and S. G. Louie, Electron correlation in semiconductors and insulators: Band gaps and quasiparticle energies, *Phys. Rev. B* 34(8), 5390 (1986)
- F. Tran and P. Blaha, Accurate band gaps of semiconductors and insulators with a semilocal exchange-correlation potential, *Phys. Rev. Lett.* 102(22), 226401 (2009)
- J. Srour, M. Badawi, F. El Haj Hassan, and A. V. Postnikov, Crystal structure and energy bands of (Ga/In)Se and $\text{Cu}(\text{In,Ga})\text{Se}_2$ semiconductors in comparison, *Phys. Status Solidi B Basic Res.* 253(8), 1472 (2016)
- Semiconductors: Data Handbook, 3rd Ed., edited by O. Madelung, Berlin: Springer, 2014
- S. Chen, X. G. Gong, and S. H. Wei, Band-structure anomalies of the chalcopyrite semiconductors CuGaX_2 versus AgGaX_2 ($X = \text{S}$ and Se) and their alloys, *Phys. Rev. B* 75(20), 205209 (2007)
- H. Mirhosseini, H. Kiss, and C. Felser, Behavior of S 3 grain boundaries in CuInSe_2 and CuGaSe_2 photovoltaic absorbers revealed by first-principles hybrid functional calculations, *Phys. Rev. Appl.* 4(6), 064005 (2015)
- A. Zunger, S. H. Wei, L. G. Ferreira, and J. E. Bernard, Special quasirandom structures, *Phys. Rev. Lett.* 65(3), 353 (1990)
- S. H. Wei, L. G. Ferreira, J. E. Bernard, and A. Zunger, Electronic properties of random alloys: Special quasirandom structures, *Phys. Rev. B* 42(15), 9622 (1990)
- G. Kresse and J. Furthmüller, Efficient iterative schemes for *ab initio* total-energy calculations using a plane-wave basis set, *Phys. Rev. B* 54(16), 11169 (1996)
- D. M. Ceperley and B. J. Alder, Ground state of the electron gas by a stochastic method, *Phys. Rev. Lett.* 45, 566 (1980)
- P. E. Blöchl, Projector augmented-wave method, *Phys. Rev. B* 50(24), 17953 (1994)
- T. Maeda and T. Wada, First-principles calculation of defect formation energy in chalcopyrite-type CuInSe_2 , CuGaSe_2 and CuAlSe_2 , *J. Phys. Chem. Solids* 66(11), 1924 (2005)
- G. Boyd, H. Kasper, and J. McFee, Linear and nonlinear optical properties of AgGaS_2 , CuGaS_2 , and CuInS_2 , and theory of the wedge technique for the measurement of nonlinear coefficients, *IEEE J. Quantum Electron.* 7(12), 563 (1971)
- B. Tell and H. M. Kasper, Optical and electrical properties of AgGaS_2 and AgGaSe_2 , *Phys. Rev. B* 4(12), 4455 (1971)
- J. Taylor, H. Guo, and J. Wang, *Ab initio* modeling of quantum transport properties of molecular electronic devices, *Phys. Rev. B* 63(24), 245407 (2001)

29. Y. B. Hu, Y. H. Zhao, and X. F. Wang, A computational investigation of topological insulator Bi_2Se_3 film, *Front. Phys.* 9(6), 760 (2014)
30. W. Ji, H. Q. Xu, and H. Guo, Quantum description of transport phenomena: Recent progress, *Front. Phys.* 9(6), 671 (2014)
31. S. H. Wei and A. Zunger, Fingerprints of CuPt ordering in III-V semiconductor alloys: Valence-band splittings, band-gap reduction, and X-ray structure factors, *Phys. Rev. B* 57(15), 8983 (1998)
32. B. Tell and P. M. Bridenbaugh, Aspects of the band structure of CuGaS_2 and CuGaSe_2 , *Phys. Rev. B* 12(8), 3330 (1975)